Analysis of acoustic emissions from cement beams when applying three-point bending with different loading rates.

A. KYRIAZOPOULOS, I. STAVRAKAS, C. ANASTASIADIS, D. TRIANTIS
Department of Electronics Engineering
Technological Educational Institute of Athens
12210, Athens
GREECE
triantis@teiath.gr http://research.ee.teiath.gr

Abstract: - This paper presents six laboratory experiments where mechanical bending load is applied on cement mortar beams at a constant rate until failure. During each experiment a constant loading rate was applied. The selected bending load rates for the experiments was ranging from 22N/s to 87N/s and the characteristic parameters of the acoustic emissions (AE) are recorded. The b-value is calculated for all of the loading stages and it is shown that the load variation has similar behavior while approaching the stages near failure. When the beams have been subjected to loading close to the 95% of their 3 point bending (3PB) strength, the cumulative energy of the AE exhibits an interesting variation in association to the loading rate. The ratio of the mean interevent time to the total number of events at each test presents a similar behavior. Conclusively, it can be asserted that for a load rate higher than 50N/s approximately leads to dynamic loading phenomena and the loading cannot be considered as quasi-static in order to evaluate the mechanical properties of the used specimens.

Key-Words: - bending, mortar, acoustic emissions, b-value analysis, cracks.

1 Introduction

The acoustic emissions (AE) recording is a widely used technique for monitoring crack growth on cement based materials [1,2]. AE are emitted as stress waves and are generated when the inner structure of a material changes due to the application of mechanical loading [1]. When a quasi-brittle material enters a fracture process, a number of AE events of different amplitudes are released. This is due to the formation and growth of micro cracks [1-3].

A typical AE signal is shown in Figure 1. In this figure several basic parameters of the AE signal are noted: the amplitude which is the highest peak voltage of the AE waveform, the counts that correspond to the number of threshold crossing pulses, the duration related to the elapsed time from the first threshold crossing to the last, and the rise time which reflects the time elapsed from the first threshold crossing to the last signal peak. The AE signal energy refers to the energy of the counts and corresponds to the measured area under the rectified signal envelope.

It is worth noting that there exists a strong relation between the AE produced from materials subjected to mechanical loading on a laboratory scale, and the seismic waves generated due to earthquakes [4,5]. This correlation has triggered broad research on AE technique aiming at its exploitation as a tool for Non-Destructive Testing (NDT). The final goal of the AE technique application is to obtain monitoring and warning for the forthcoming failure in engineering materials as well as in rocks [6].

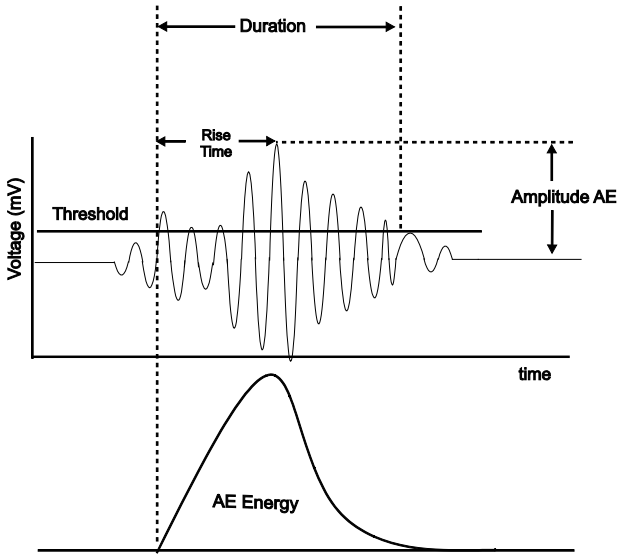

Fig. 1: Parameters of a typical AE signal

Extended research work has been conducted mostly focusing on the correlation of the fracture process of

cement based materials to the AE properties [1]. Given that the AE peak amplitude is associated with the magnitude of fracture, the fracture process can be studied through the AE amplitude distribution analysis. This is known as the "b-value analysis", whereas in seismology the b-value is defined as the negative slope of the semi-logarithmic plot between earthquake frequency and its magnitude [7].

The aim of the present work is to establish the behavior of the b-value during laboratory experiments of 3-point bending (3PB) on cement beams, following to the application of constant-rate loading until failure (ultimate load). A series of laboratory experiments have been carried out, applying different load rates in order to investigate whether the load rate differentiates the type of the b-value fluctuation, as the studied material passes through the different stages from the microscopic towards the macroscopic fractures.

2 b-value Analysis

The b-value analysis constitutes a popular method used for damage quantification. The b-value was originally defined in seismology. The question was whether it was possible to apply AE signals in engineering materials. Initially, the AE technique was applied in order to evaluate damage in concrete beam [8]. In the case of the AE technique, the Gutenberg-Richter relationship between cumulative frequency and magnitude is given by the equation:

$$log_{10}N(M) = a - b \cdot \left(\frac{A_{dB}}{20}\right) \quad \text{Eq. 1}$$

where A_{dB} is the peak amplitude, N is the number of AE events with amplitude greater than the threshold, M is magnitude of the events, α is an empirical parameter and b is the AE based b-value [8].

An alternative of calculating the b-value is by using the Aki's method [9] which has been applied for the study of the fracture process in rocks [10,11]. According to Aki's method, the b-value is calculated by the relationship:

$$b = \frac{20log_{10}e}{<\alpha>-\alpha_c} = \frac{8.686}{<\alpha>-\alpha_c} \quad \text{Eq. 2}$$

where <a> is the mean amplitude and a_c is the threshold amplitude in dB.

Given that during a loading test towards failure the amplitude distribution of the AE is modified, statistical values (i.e. mean and standard deviation) of a certain number (n) of AE events can be taken into account in order to obtain an "improved b-value" (I_b). This improved value has been defined as follows [12,13]:

$$I_b = \frac{logN(\mu+\alpha_1\sigma)-logN(\mu-\alpha_2\sigma)}{(\alpha_1+\alpha_2)\sigma} \quad \text{Eq. 3}$$

where μ is the mean amplitude, σ the standard deviation and α_1 and α_2 are user-defined constants. Usually, $\alpha_1=\alpha_2=1$. In order to compare the Ib-value to the corresponding seisimic b-value, the Ib-value of equation 3, should be multiplied by 20 [13]. A standard number (n) of successive events can be used for the estimation of the Ib-value which might range between 50 and 100 [14].

3 Experimental procedure

Ordinary Portland cement (OPC) was used for producing the cement mortar specimens (beams), which were subjected to bending test. The mixture included cement, sand, (fine aggregates) and water at a weight ratio of 1:3:0.5 respectively. Further details on the preparation of the specimens are presented in an earlier paper [15]. In the present study, the dimensions of the beams were 200 mm long, with a square cross- section of 50 mm x 50 mm. The beams were used for bending tests 90 days after their preparation, thus allowing them to reach a quite high percent of their total strength [16].

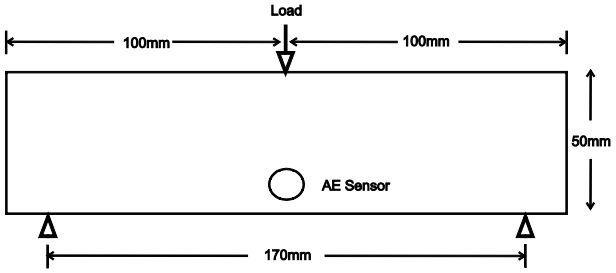

Fig. 2: Schematic diagram of beam geometry

The beams were loaded in 3-point bending and the support span was 170 mm as presented in Figure 2. Preliminary tests indicated that the strength of the beams ranged between 2.9 and 3.1 kN. In the current study 6 experiments of constant-rate increase of the bending load were conducted. For each laboratory test the loading rate was different, specifically, the following six rates were applied: 22N/s, 34N/s, 44N/s, 53N/s, 67N/s and 87N/s.

During the tests the released AE events beams were monitored using a Physical Acoustic Corporation (PAC) Mistras Systems. The AE sensor was installed at the center of the beam (see Figure 2) in order to ensure that it is installed at a region where main damages occur due to the bending. The AE

ISBN: 978-1-61804-316-0

threshold for detecting acoustic events was set at 45dB during all the six tests. This threshold value was selected in order to minimize the reflected AE signals due to the limited dimensions of the used specimens. Further details on the monitoring of the AE are described in an earlier paper [17,18].

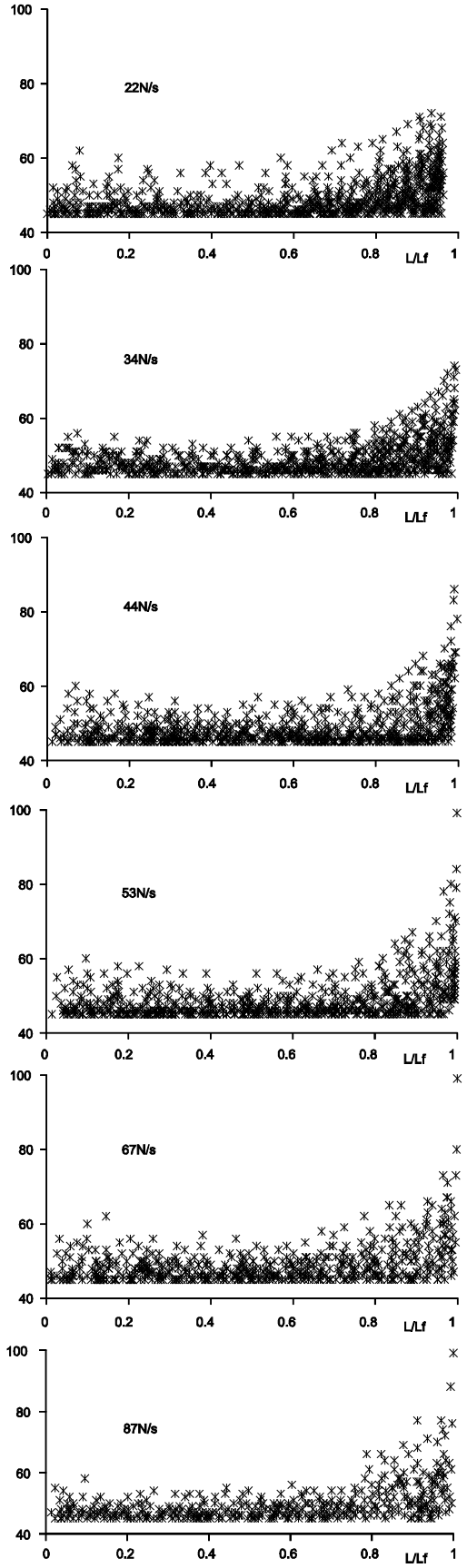

Fig. 3: The discrete values of the AE amplitudes with respect to the normalized applied load for all the six conducted experiments.

ISBN: 978-1-61804-316-0

4 Analyses and Results

Figure 3 depicts the amplitude values of the AE events in dB, recorded for all six loading tests from the beginning of loading up to failure of the beams. The horizontal axis represents the normalized load L/L_f where L is the load value and L_f is the 3PB strength of each beam.

Table 1 shows the AE events total number N up to the failure of each beam for all six tests. In the same table the 3PB strength of each beam is also recorded. It is clear that as the loading rate increased, the total number of recorded AE events, N, decreased. Another interesting observation was that the mean amplitude (<a>) of the N events in all tests decreases as the loading rate increases but shows a tendency to increase when the rate exceeds 80N/s (see table 1).

Table 1. The basic mechanical and AE parameters for the conducted experiments.

Another quantity measured was the "interevent times" ($\delta\tau$) of the recorded AE. The mean value of the interevent times ($<\delta\tau>$), was calculated for each one of the six loading tests (see Table 1) and it seems clear that as the load rate increases, the mean interevent times decrease with a tendency to be stabilized for rates greater than 60N/s (see Table 1).

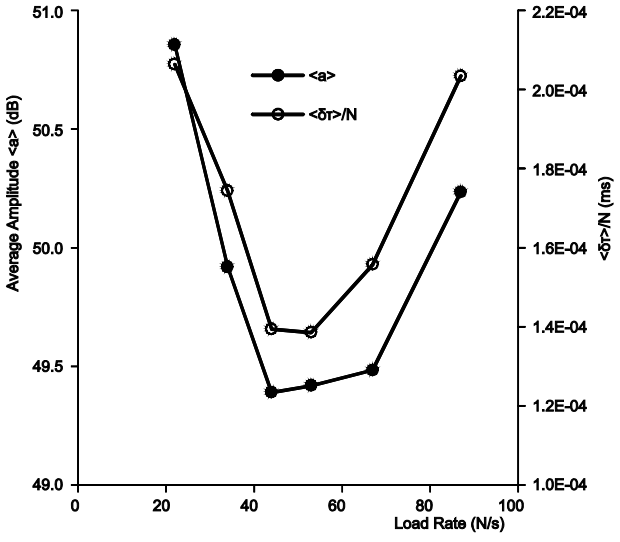

Fig. 4: Variation of the mean amplitude and the ratio $<\delta\tau>/N$ with respect to the loading rate.

It is interesting to notice that the ratio $<\delta\tau>/N$ shows a similar behavior to that of the mean amplitude $<\alpha>$ in correlation to the load rate (see Figure 4).

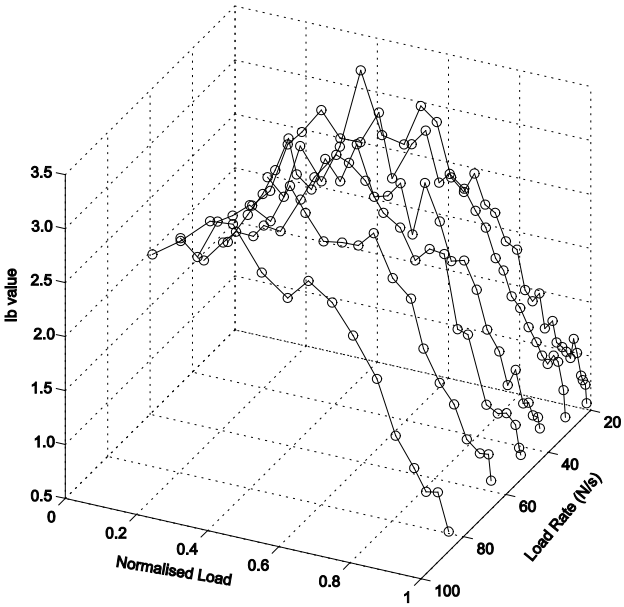

Fig. 5: Variation Ib-value with L/L_f for all the six tests.

loading rate (N/s)	N events	strength L_f (kN)	<a>	$<\delta\tau>$
22	805	2.94	50.85	0.166
34	722	3.10	49.92	0.126
44	702	3.06	49.39	0.098
53	633	2.98	49.42	0.088
67	529	2.95	49.48	0.082
87	397	2.90	50.23	0.081

In order to show up the variability of the I_b-value, during a load test for each one of the six tests, the whole set of AE events were separated in groups of successive events. Every group consisted of k=50 events. Consequent I_b-values were calculated by shifting the group for 25 events. Thus, for each group, the former 25 events belonged to the previous group while the latter 25 events belonged to the next group. The calculated I_b-values corresponded to the normalized load (L/L_f) where L corresponded to the fiftieth (50^{th}) event of each group. According the Eq. 3 the parameters $\alpha_1=\alpha_2=1$. The results are shown as I_b-values versus L/L_f in the 3D plot of Figure 5 for all the six conducted experiments. It is evident that during the early stages of loading the I_b-values exhibit a noticeable increase indicating prevalence of microcracks [19].

For all tests high I_b-values (I_b between 2.5 and 3.2) exist in the region L/L_f =0.45±0.15 due to a large number of small AE events. This is related to new crack formation and the consequent slow crack growth [6]. For L/L_f >0.8 the I_b-values start to decrease intensely exhibiting values lower than 2. For L/L_f >0.9 in all tests regardless of the loading rate the I_b-values drop below 1.5 reaching values

between 0.7 and 0.8 in the failure region of the beams.

This is indicative of unstable crack growth given that relatively high amplitude AE events are observed in large numbers. It is characteristic that the variability of the I_b-value during the 3PB loading tests, obtains no significant differences with the loading rate. It is worth to notice that in the 6th test where the loading rate is high (87N/s) it seems that the first stage that corresponds to new crack formation is limited up to a normalized load not exceeding 0.4.

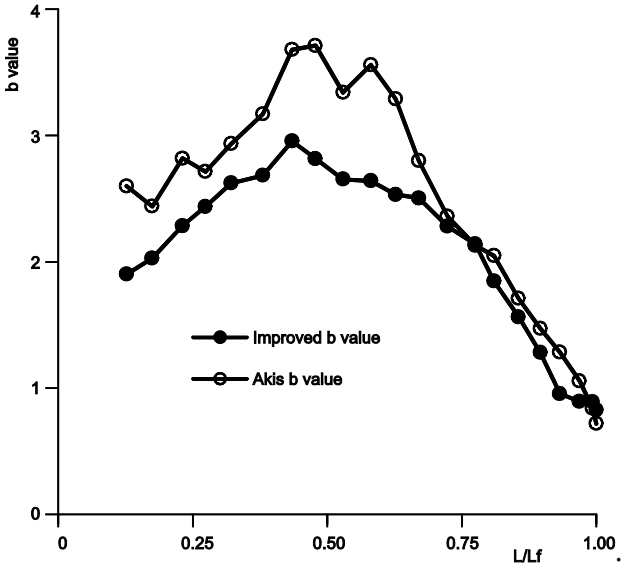

Fig. 6: Comparative curves of the variation between the b-value (Aki' s method) and the I_b-value (I_b) during the experiment with loading rate 67N/s.

If the Eq. 2 (Aki's method) is reclaimed, the resulting b-values are slightly higher than the I_b-values especially in the primary loading stages which has been observed by other researchers [2]. Figure 6 depicts an indicative variation of b-values (Aki's method) and I_b-values versus L/L_f during the 3PB test with 67N/s loading rate. It is obvious that for L/L_f >0.7 there is a better value coincidence. A similar behavior is found for all the conducted experiments.

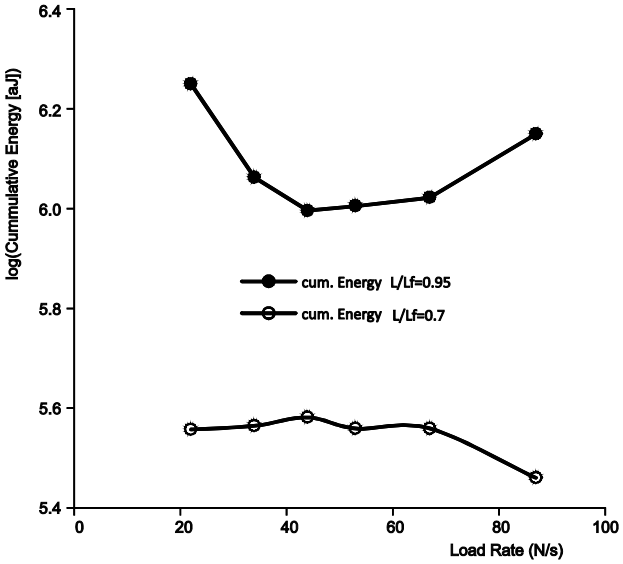

Fig. 7 Cumulative AE energy versus load rate on stages L/L_f = 0.70 and 0.95

Finally, the cumulative counts' AE energy was calculated during all the loading stages for each of the conducted experiments up to the failure of the specimens. In order to compare the cumulative Energy values for each tests the cumulative AE energy was estimated for two stages. The first stage corresponded to 3PB load up to 70% of the strength of each beam where the crack growth processes are not initiated. The second one corresponded to high load values (95%) with respect to the strength of the specimen where instable crack growth mechanisms take place. The decimal logarithm of the cumulative energies for both the above stages for each load rate are presented in Figure 7. For the stage L/L_f=0.70 up to a loading rate 70N/s approximately the cumulative energy is relatively stable. Contrary to that for the stage L/L_f=0.95 a clear variation may be seen where the edge values of loading rates (i.e. 22N/s and 87N/s) show increased cumulative energy values (see

Figure 7). A similar behavior is also obtained for the corresponding variations of the quantities <a> and <δτ>/N (see Figure 4). This fact constitutes indication for the separation between quasi-static and dynamic loading. Such behavior clearly show up that there is a measurable quantity to investigate if the rate of applied mechanical load influences the mechanical behavior of a specimen under Three Point Bending loading.

4 Conclusion

Taking into consideration the above results the following major conclusions can be drawn.

ISBN: 978-1-61804-316-0

The Acoustic Emissions detection technique constitutes a valuable tool that directly provides information regarding the mechanical status of a material. Provided, that the fracture phenomena are mainly studied under the concept of numerical modeling and destructive testing experimental techniques such novel techniques, like the AE, may be implemented in field measurements and are rapidly adopted be the scientific and engineering communities.

The b-value analysis of the Acoustic Emissions, has shown that regardless the loading rate of the cement mortar beams the I_b-value fluctuations are relatively large and more frequent in the initiation stage. Such fluctuations may be attributed to the nature of the AE sources and specifically the mode of the micofracture or even to distinguish new microcrackings from crack growth processes. Additionally, the high degree of fluctuations clearly indicated a non-organized situation that is mainly controlled by the characteristics of the used specimens.

The nucleation stage clearly initiates when the applied mechanical load is higher than 70% of the Three Point Bending strength of the specimens. During this region the microfractue phenomena start to interact guiding the forming the necessary conditions of fracture.

The cumulative energy and the ratio: (interevent times)/(total number of recorded AE events) clearly show a variability with respect to the loading rate that is applied on the cement mortar beams.

Acknowledgements:

This research has been co-financed by the European Union (European Social Fund—ESF) (no. MIS 379389) and Greek national funds through the Operational Program ‘‘Education and Lifelong Learning’’ of the National Strategic Reference Framework (NSRF)—Research Funding Program: ARCHIMEDES III. Investing in knowledge society through the European Social Fund.

References:

[1] Ohtsu, M., Tomoda, Y.. Phenomenological model of corrosion process in reinforced concrete identified by acoustic emission. *ACI Mater J.* 105(2), 2008, pp. 194–199.

[2] Sagar RV, Prasad BKR, Kumar SS, An experimental study on cracking evolution in concrete and cement mortar by the b-value analysis of acoustic emission technique, *Cement and Concrete Research*, 42 (8) 2012, pp. 1094-1104.

[3] Sagar RV, Prasad BKR, Damage limit states of reinforced concrete beams subjected to incremental cyclic loading using relaxation ratio analysis of AE parameters, *Construction and Building Materials* 35, 2012, pp. 139-148.

[4] Lockner, D., The role of acoustic emission in the study of rock fracture. *Int. J. Rock Mech. Min. Sci. Geomech. Abstr*., 1993, 30, pp. 883–899

[5] Lockner, D., Brittle fracture as an analog to earthquakes: Can acoustic emission be used to develop a viable prediction strategy, *J. Acoust. Emission*, 14, 1996, pp. S88–S101

[6] Rao, M.V.M.S. and Prasanna Lakshmi, K.J.,. Analysis of b-value and improved b-value of acoustic emissions accompanying rock fracture. *Cur. Sci*, 89, 2005, pp. 1577-1582.

[7] Main, I.G., Meredith, P.G and Jones, C., A reinterpretation of the precursory seismic b-value anomaly from fracture mechanics, *Geoph. J. Int*., 96, 1989, pp. 131–138.

[8] Colombo, I.S., Main, I.G. and Ford, M.C., Assessing damage of reinforced concrete beam using b-value analysis of acoustic emission signal. *J. Mat. Civ. Eng*., 15, 2003, pp. 280–286.

[9] Aki, K., Maximum likelihood estimates of b in the formula logN=a–bm and its confidence limits. Bull. Earthquake Res. Inst., Tokyo Univ., 43, 1965, pp. 237–239.

[10] Main, I. G., P. G. Meredith, and C. Jones, A reinterpretation of the precursory seismic b-value anomaly from fracture mechanics, *Geoph. J. Int*., 96, 1989, pp. 131–138.

[11] Cox, S.J.D. and Meredith, P.G., Microcrack formation and material softening in rock measured by monitoring acoustic emission, Int. *J. Rock Mech. Min. Sci. and Geomech. Abstr*., 30(1), 1993, pp. 11-24.

[12] Shiotani, T., Fujii, K., Aoki, T. Amou, K., Evaluation of progressive failure using AE sources and improved b-value on slope model tests. *Prog. Acoust. Emission*, VII, 1994, pp. 529–534.

[13] Shiotani, T., Yuyama S., Li, Z.W., Ohtsu, M., Application of the AE improved b-value to qualitative evaluation of fracture process in concrete materials, *J. Acoust. Emission*, 19, 2001, pp.118–132.

[14] Kaphle, M.R. Tan, A., Thambiratnam, D., Chan T.H.T., Damage quantification techniques in

acoustic emission monitoring, in *WCEAM 2011 Sixth World Congress on Engineering Asset Management*, 2011.

[15] Kyriazopoulos, A., Anastasiadis, C., Triantis, D., Brown, J.C., Non-destructive evaluation of cement-based materials from pressure-stimulated electrical emission - Preliminary results, *Construction and Building Materials*, 25, 2011, pp. 1980–1990.

[16] Kosmatka, S.H., Kerkhoff, B., Panarese W.C., Design and control of concrete mixtures, *Portland Cement Association*, 2002, 14th ed.

[17] Stergiopoulos, C., Stavrakas, I., Hloupis, G., Triantis, D., Vallianatos, F., Electrical and acoustic emissions in cement mortar beams subjected to mechanical loading up to fracture, *Engineering Failure Analysis*, 35, 2013 pp. 454–461.

[18] Stergiopoulos, C., Stavrakas, I., Hloupis, G., Kyriazopoulos, A., Triantis, D., Anastasiadis, C., Stonham, J., Nondestructive Testing Electrical Methods for Sensing Damages in Cement Mortar Beams, *Open Journal of Applied Sciences*, 3, 2013, pp 50-55.

[19] Rouchier, S., Janssen, H., Rode, C. Woloszyn, M., Foray, G., Jean-Jacques Roux, J.J., Characterization of fracture patterns and hygric properties for moisture flow modelling in cracked concrete. Constr. Build. Mater., 34, 2012, pp. 54–62.

ISBN: 978-1-61804-316-0